POLITECNICO DI TORINO
Repository ISTITUZIONALE

Identification of a UR5 collaborative robot dynamic parameters

Original
Identification of a UR5 collaborative robot dynamic parameters / Raviola, A.; De Martin, A.; Guida, R.; Pastorelli, S.; Mauro, S.; Sorli, M.. - 102:(2021), pp. 69-77. (Intervento presentato al convegno RAAD 2021: The 30th International Conference on Robotics in Alpe-Adria-Danube Region) [10.1007/978-3-030-75259-0_8].

Availability:
This version is available at: 11583/2901812 since: 2021-05-19T18:22:32Z

Publisher:
Springer

Published
DOI:10.1007/978-3-030-75259-0_8

Terms of use:

This article is made available under terms and conditions as specified in the corresponding bibliographic description in the repository

Publisher copyright
Springer postprint/Author's Accepted Manuscript

This version of the article has been accepted for publication, after peer review (when applicable) and is subject to Springer Nature's AM terms of use, but is not the Version of Record and does not reflect post-acceptance improvements, or any corrections. The Version of Record is available online at: http://dx.doi.org/10.1007/978-3-030-75259-0_8

(Article begins on next page)

12 October 2024

Identification of a UR5 Collaborative Robot Dynamic Parameters

Andrea Raviola[1], Andrea De Martin[1], Roberto Guida[1], Stefano Pastorelli[1], Stefano Mauro[1] and Massimo Sorli[1]

[1] Politecnico di Torino, Department of Mechanical and Aerospace Engineering, Corso Duca degli Abruzzi 24, 10129, Torino, Italy
andrea.raviola@polito.it

Abstract. The present paper describes an algorithm for the identification of the dynamic parameters of an industrial robot. This approach is based on the possibility to write robot dynamics in a linear form with respect to a specific set of dynamic parameters. To properly detect them, the coefficients of a 5th order Fast Fourier Series (FFS) trajectory have been optimized using a genetic algorithm. Such identification trajectory has been then commanded to a UR5 collaborative robot from Universal Robots and experimental joints torques have been recorded at a frequency of 125 Hz. Base dynamic parameters were identified using least square errors optimization reaching low standard deviations. The algorithm has been validated with a second persistent trajectory with good results. Temperature effects on friction coefficients have been analyzed by running two identification processes: one just after the first power up of the robot and the other one after a half an hour warm up.

Keywords: Industrial Robots, Collaborative Robotics, Dynamic Modeling, Parameter Identification, High-Fidelity Modeling.

1 Introduction

High-fidelity (HF) models of industrial robots can be used to predict the behavior of a manipulator for different tasks and operating conditions. Moreover, recent researches, like [1], [2], and [3], highlighted how mathematical models might have a key role for failure detection and prediction in several mechanical and electrical systems. In this framework, a deep knowledge of the robot under analysis is needed to carry out reliable simulations based on a model customized on a specific machine. Nevertheless, as it often happens in industry, while the kinematic parameters of a manipulator are usually provided by the manufacturer, the same does not apply to the dynamic ones. As an example, Universal Robots provides, for UR cobots, only 4 out of 13 dynamic parameters for each joint/link: mass and position of the center of mass. Even URSim, the official offline simulator developed by Universal Robots, does not take into account all of them. As a consequence, under the same input trajectories, torques predicted by any model of the manipulator could be very different from the ones measured from the robot itself. This could lead to a wrong evaluation of the power used by the robot during a

specific application or to a not reliable assessment of the risks related to a collaborative robotics application such as a collision between the cobot and the human operator, that could cause severe accidents in those cases in which anticollision algorithms are used to modify the trajectory in real time to react to the motion of the operator, as reported in [4-6].

To overcome these limitations, the present research provides an algorithm able to identify the dynamic parameters of an industrial manipulator. The proposed approach has been validated with a UR5 collaborative robot.

2 Mathematical Model of the UR5 Collaborative Robot

For an industrial robot, the inverse dynamics formulation can be derived using Euler's equations or a Lagrangian-based approach [7]. So, for a *n*-dof (degrees of freedom) manipulator, at a given instant *k*, it is possible to write:

$$\boldsymbol{M}(\boldsymbol{q})\ddot{\boldsymbol{q}} + \boldsymbol{C}(\boldsymbol{q},\dot{\boldsymbol{q}})\dot{\boldsymbol{q}} + \boldsymbol{F}(\dot{\boldsymbol{q}}) + \boldsymbol{G}(\boldsymbol{q}) = \boldsymbol{\tau} \tag{1}$$

where $\boldsymbol{M}(\boldsymbol{q}) \in \mathbb{R}^{n\times n}$ is the symmetric positive definite mass matrix, $\boldsymbol{C}(\boldsymbol{q},\dot{\boldsymbol{q}}) \in \mathbb{R}^{n\times n}$ is the Coriolis and centripetal coupling matrix, $\boldsymbol{F}(\dot{\boldsymbol{q}}) \in \mathbb{R}^{n}$ is the friction force vector, $\boldsymbol{G}(\boldsymbol{q}) \in \mathbb{R}^{n}$ is the gravitational force vector, $\boldsymbol{\tau} \in \mathbb{R}^{n}$ is the joints torques vector while $\boldsymbol{q},\dot{\boldsymbol{q}},\ddot{\boldsymbol{q}} \in \mathbb{R}^{n}$ are, respectively, the joints angular positions, velocities, and accelerations.

However, for the purpose of this research, it is necessary to rewrite Eq. (1) in a linear form with respect to a set of properly defined dynamic parameters $\boldsymbol{p} \in \mathbb{R}^{13n}$ as:

$$\boldsymbol{Y}\cdot\boldsymbol{p} = \boldsymbol{\tau} \tag{2}$$

where $\boldsymbol{Y} \in \mathbb{R}^{n\times 13n}$ is the *regression matrix* or *regressor*. More in detail, for a generic trajectory point *k*, Eq. (2) has the structure reported in Eq. (3):

$$\begin{bmatrix}\boldsymbol{Y}_{id}{}^{(k)} & \boldsymbol{Y}_{c}^{(k)} & \boldsymbol{Y}_{v}^{(k)} & \boldsymbol{Y}_{I,m}^{(k)}\end{bmatrix}\begin{Bmatrix}\boldsymbol{p}_{id}\\ \boldsymbol{p}_{c}\\ \boldsymbol{p}_{v}\\ \boldsymbol{p}_{I,m}\end{Bmatrix} = \boldsymbol{\tau}^{(k)} \tag{3}$$

where $\boldsymbol{Y}_{id}{}^{(k)} \in \mathbb{R}^{n\times 10n}$ is the regressor block built from the Lagrange motion equations according to [8]. In addition, for a complete model of the manipulator, Coulomb and viscous friction phenomena are described, for each joint *i*, by, respectively: $\boldsymbol{Y}_{c}{}^{(k)} = diag\left(tanh\left(\frac{\dot{q}_i}{0.001}\right)\right) \in \mathbb{R}^{n\times n}$ and $\boldsymbol{Y}_{v}{}^{(k)} = diag(\dot{q}_i) \in \mathbb{R}^{n\times n}$. The effects of motors inertia have been implemented in $\boldsymbol{Y}_{I,m}{}^{(k)} = diag(\ddot{q}_i) \in \mathbb{R}^{n\times n}$. Similarly, $\boldsymbol{p}$ is composed by $\boldsymbol{p}_{id} = [\boldsymbol{p}_{id,1},\boldsymbol{p}_{id,2},\boldsymbol{p}_{id,3},\boldsymbol{p}_{id,4},\boldsymbol{p}_{id,5},\boldsymbol{p}_{id,6}]^T \in \mathbb{R}^{10n}$ where, for the single body i, $\boldsymbol{p}_{id,i} = [m, mx, my, mz, J_{xx}, J_{yy}, J_{zz}, J_{yz} = J_{zy}, J_{xz} = J_{zx}, J_{xy} = J_{yx}]_i \in \mathbb{R}^{10}$, which contains the information about its mass, the position of the center of mass according to the x_i, y_i and z_i axes and its moments of inertia. The Coulomb and viscous coefficients have been grouped inside $\boldsymbol{p}_c = [f_{c1}, f_{c2}, f_{c3}, f_{c4}, f_{c5}, f_{c6}] \in \mathbb{R}^6$ and

$\boldsymbol{p}_v = [f_{v1}, f_{v2}, f_{v3}, f_{v4}, f_{v5}, f_{v6}] \in \mathbb{R}^6$, while the motor inertia of each joint are stored in $\boldsymbol{p}_{I,m} = G^2 \cdot [I_{m1}, I_{m2}, I_{m3}, I_{m4}, I_{m5}, I_{m6}] \in \mathbb{R}^6$ respectively, where G is the gear ratio.

2.1 Regressor Reduction

Since not all the manipulator dynamic parameters are linearly independent, it is necessary to remove from the regressor $\boldsymbol{Y}$ all the null columns to create a reduced matrix $\boldsymbol{Y}_B$ with mutually independent columns, so that $\boldsymbol{Y}_B \cdot \boldsymbol{p}_B = \boldsymbol{\tau}$, where $\boldsymbol{p}_B$ is the *base dynamic parameter* vector. To do this, two numerical approaches are commonly used: QR decomposition and Singular Value Decomposition (SVD). As in [9], the symbolic regressor $\boldsymbol{Y} \in \mathbb{R}^{n \times 13n}$ is evaluated using 25 random values of angular positions, velocities, and accelerations. Each single regressor is stacked to form $\overline{\boldsymbol{Y}}_{25} \in \mathbb{R}^{25n \times 13n}$. By applying the SVD reduction, $\overline{\boldsymbol{Y}}_{25}$ is written as $\overline{\boldsymbol{Y}}_{25} = \boldsymbol{U\Sigma V^T}$, where $\boldsymbol{\Sigma} = \mathrm{diag}(\sigma_i) \in \mathbb{R}^{13n \times 13n}$ is a diagonal matrix whose elements are the singular values σ_i of $\overline{\boldsymbol{Y}}_{25}$, reported in Fig. 1(a).

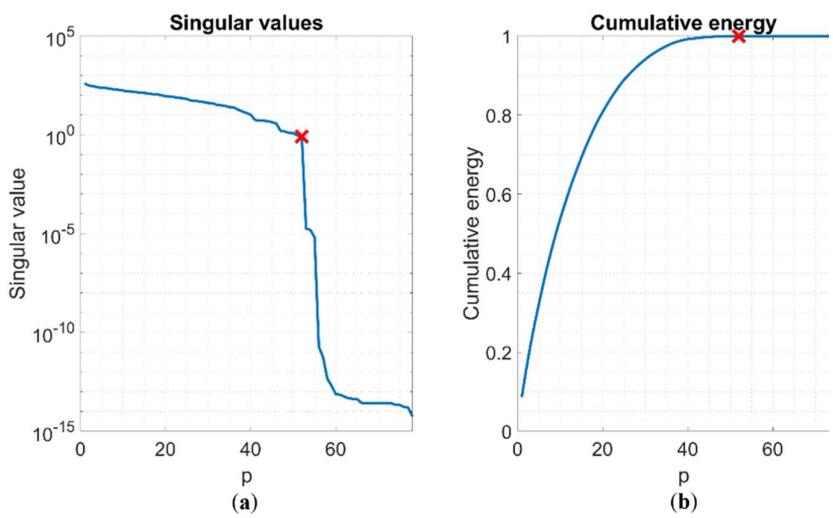

Fig. 1. (**a**) Singular values of the $\overline{\boldsymbol{Y}}_{25}$ matrix as a function of the number of the dynamic parameters $\boldsymbol{p}$; (**b**) Cumulative energy of the $\overline{\boldsymbol{Y}}_{25}$ matrix.

This analysis highlights how, in order to describe the 100% of the cumulative energy of the system [10], shown in Fig. 1(b), it is necessary to choose 52 base dynamic parameters. This information is used to check the quality of the QR decomposition adopted to reduce the system from $\boldsymbol{Y} \in \mathbb{R}^{6 \times 78}$ to $\boldsymbol{Y}_B \in \mathbb{R}^{6 \times 52}$ and from $\boldsymbol{p} \in \mathbb{R}^{78}$ to $\boldsymbol{p}_B \in \mathbb{R}^{52}$. As a result, among all the aforementioned 78 dynamic parameters of the UR5 (13 for each joint), only 30 are totally identifiable, 39 are identifiable with linear dependency, while the remaining 9 do not contribute to the dynamics of the manipulator, so they cannot be identified.

2.2 Excitation Trajectory

For a proper identification of $\boldsymbol{p}_B$, the UR5 has been commanded with a trajectory built using a 5th order Finite Fourier Series (FFS) as suggested by [11–13]. Alternatives to FFS could be found in [14] and [15], where a 5th order polynomial is used, or in [16] in which a B-splines have been selected. Angular positions, for each joint *i*, are calculated according to Eq. (4):

$$q_i(t) = q_{i,0} + \sum_{l=1}^{5} a_{i,l}\, sin(\omega_f lt) - b_{i,l}\, cos(\omega_f lt) \tag{4}$$

where:

- ω_f is the fundamental frequency, equal for each joint in order to guarantee the periodicity of the robot movements. It is defined as $\omega_f=2\pi T$, where T is the identification trajectory period set to 10 s;
- $q_{i,0}$ is the joint position offset. According to the robot mounting configuration adopted during the experimental campaign, it is equal to [0, -π/2, 0, 0, 0, 0] rad;
- $a_{i,l}$ and $b_{i,l}$ are the coefficients of the FFS that have to be found by optimization in order to define a persistent identification trajectory able to continuously excite all the identifiable dynamic parameters.

Since the UR5 must be able to execute the identification trajectory, physical constraints of the manipulator and of the test bench, on which the robot is mounted, have been implemented by adapting the non-linear constraints described in [17]. These limits have been chosen both according to the mechanical constraints of the robot ($\dot{q}_{max}$ and $\ddot{q}_{max}$ are equal to π rad/s and 5.5π rad/s^2 respectively) and to avoid any self-collision of the robot or with the environment by setting q_{max} = [2π, π, π, 2π, 2π, 2π] rad.

Moreover, to prevent high vibrations or unexpected behaviors at the start and end points of the commanded trajectory, the initial and final values of angular velocities and accelerations of each joint have been imposed to be 0.

The FFS coefficients $a_{i,l}$ and $b_{i,l}$ have been identified using the MATLAB Global Optimization Toolbox. In particular, due to the large dimension of the problem, a genetic algorithm (GA) has been used as proposed by [18] and [19]. According to [20], several cost functions could be used as the objective function to be minimized by GA, such as the one in Eq. (5) used in the present work:

$$\min_{\boldsymbol{q},\dot{\boldsymbol{q}},\ddot{\boldsymbol{q}}} cond\left(\overline{\boldsymbol{Y}}_B(\boldsymbol{q},\dot{\boldsymbol{q}},\ddot{\boldsymbol{q}})\right) \tag{5}$$

where $\overline{\boldsymbol{Y}}_B = \begin{pmatrix} \boldsymbol{Y}_{B,1} \\ \vdots \\ \boldsymbol{Y}_{B,N_id} \end{pmatrix} \in \mathbb{R}^{(n\times N_id)\times 52}$ is the *observation matrix* built by piling up the single regressors $\boldsymbol{Y}_{B,k}$ for each single trajectory point *k* of the identification trajectory. To solve the constrained non-linear optimization problem, a population of 300 individuals has been used in the GA and, after five generations, the algorithm converged to a solution returning a condition number of 153. The resulting angular positions commanded to the UR5 are reported in Fig. 2.

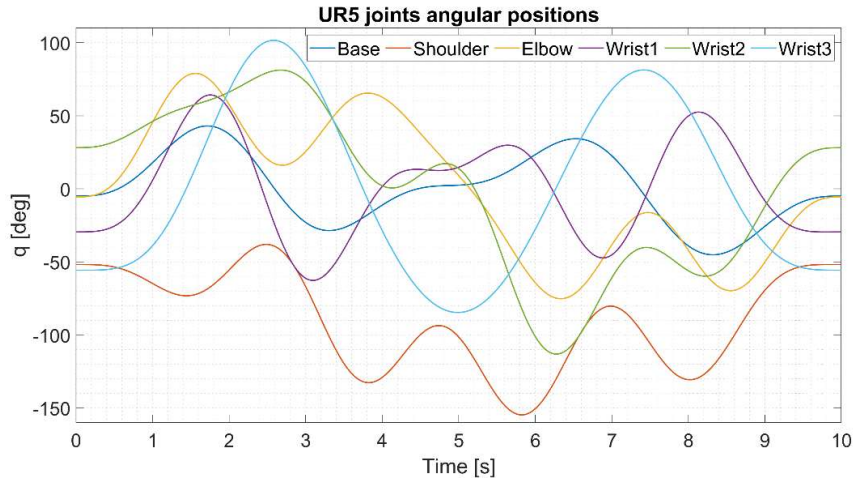

Fig. 2. Angular positions of the UR5 joints during one period of the identification trajectory.

To prevent an ill-conditioning of the observation matrix $\overline{\boldsymbol{Y}}_B$, the identification trajectory has been repeated three times. To execute both the identification and the validation trajectories, the *servoj* function, developed by Universal Robots, has been adopted using a *lookahead time* and a *gain* of 0.03 and 500 respectively to avoid any vibration of the robot arm.

3 Results

Since the UR5 provides only the angular positions and velocities of the joints at each trajectory point *k*, while the regressor also needs the values of the angular accelerations to estimate the joints torques, it has been necessary to calculate them by numerical derivation. This operation, however, could amplify the noise of the data, so a filter has been adopted as suggested by [9] and [11].

Moreover, the robot used in the experimental campaign is not provided with torque sensors on its joints, so these values have been calculated by multiplying motor currents, gear ratio, and torque constants K_t. For the robot used in the experimental campaign, the gear ratio is 101, while the values of K_t, equal to [0.1350 0.1361 0.1355 0.0957 0.0865 0.0893] Nm/A, are provided by the manufacturer.

The base dynamic parameters are obtained through the UR5 torques $\overline{\boldsymbol{\tau}}_{ID} = \begin{pmatrix} \boldsymbol{\tau}_{ID,1} \\ \vdots \\ \boldsymbol{\tau}_{ID,N_id} \end{pmatrix}$ measured during the identification trajectory, by using the least square errors optimization:

$$\boldsymbol{p}_B = (\overline{\boldsymbol{Y}}_B^T \cdot \overline{\boldsymbol{Y}}_B)^{-1} \cdot \overline{\boldsymbol{Y}}_B^T \cdot \overline{\boldsymbol{\tau}}_{ID} \tag{6}$$

An alternative method to Eq. (6), which takes into account the different joint sizes of the manipulator joints, is proposed in [9].

3.1 Algorithm Validation

To validate the proposed algorithm, a second persistent trajectory has been commanded to the UR5 and the predicted torques have been calculated using the reduced regressor and the identified base dynamic parameters. An example of the results obtained with the validation trajectory for the UR5 elbow (joint 3) is reported in Fig. 3.

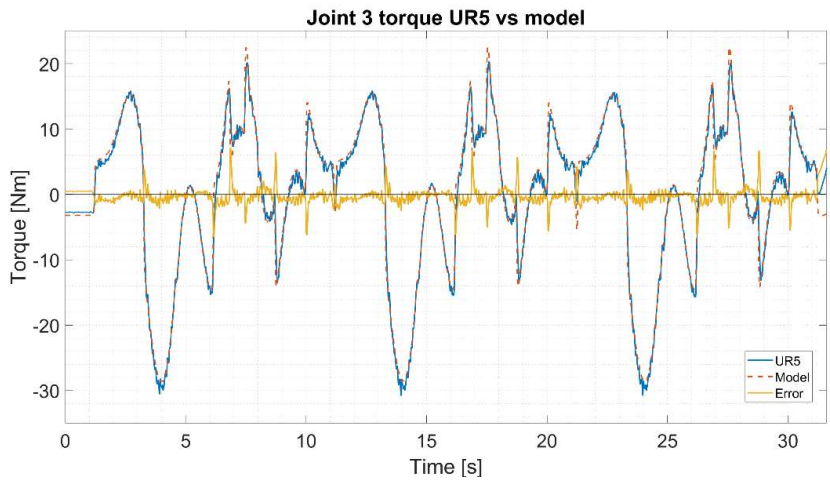

Fig. 3. Measured and predicted torques of the UR5 elbow for the validation trajectory.

Since the described model does not take into account the static friction of the robot, there could be higher errors among the predicted torques and the measured ones when the manipulator does not move.

To better evaluate the goodness of the proposed algorithm, the normalized error, defined as: $e_N = \frac{1}{N_val}\sqrt{\boldsymbol{e}^T \cdot \boldsymbol{e}}$ can be calculated, where $\boldsymbol{e} = \overline{\boldsymbol{Y}}_B \boldsymbol{p}_B - \overline{\boldsymbol{\tau}}_{UR5}$ with $\overline{\boldsymbol{Y}}_B = \begin{pmatrix} \boldsymbol{Y}_{B,1} \\ \vdots \\ \boldsymbol{Y}_{B,N_val} \end{pmatrix}$ and $\overline{\boldsymbol{\tau}}_{UR5} = \begin{pmatrix} \boldsymbol{\tau}_{UR5,1} \\ \vdots \\ \boldsymbol{\tau}_{UR5,N_val} \end{pmatrix}$ being the measured torques for each point k of the validation trajectory. In the proposed example, the normalized errors e_N is equal to 0.0550.

3.2 Effect of Temperature on Dynamic Parameters

In order to understand the effect of friction on the results, the impact of joints temperature on the estimate of the base dynamic parameters $\boldsymbol{p}_B$ has been considered. To do so, the identification trajectory reported in Fig. 2 has been commanded to the UR5, first just after its power up (cold robot) and then, after 30 minutes of high dynamic

movements (warm robot). The temperature of the UR5 joints in the two working conditions have been registered to be:

- **Cold robot**: T = [24.0, 24.0, 21.1, 24.7, 21.5, 22.5] °C;
- **Warm robot**: T = [33.8, 31.6, 29.8, 35.1, 36.8, 37.2] °C.

The results are reported in Fig. 4, where it can be noticed that all the base dynamic parameters whose values should not be affected by temperature ($\boldsymbol{p}_B(1) - \boldsymbol{p}_B(36)$ and $\boldsymbol{p}_B(49) - \boldsymbol{p}_B(52)$) are nearly the same in both working conditions. On the other hand, there are differences in the friction parameters ($\boldsymbol{p}_B(37) - \boldsymbol{p}_B(48)$), in particular in the ones related to viscous friction ($\boldsymbol{p}_B(43) - \boldsymbol{p}_B(48)$), where it has been registered a reduction of up to 35%. This test highlights how temperature affects the viscosity of the grease used to lubricate the joints and proves the stability of the proposed identification algorithm.

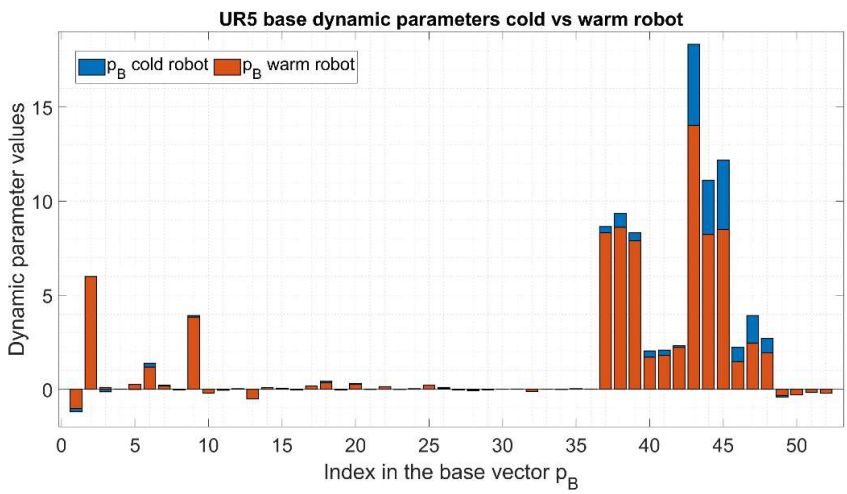

Fig. 4. Values of the dynamic parameters of the UR5 collaborative robot just after its power up (cold robot) and after a half an hour warm up (warm robot).

4 Conclusions

In this paper, a method for dynamic parameters identification of an industrial robot has been described and tests have been run using a UR5 collaborative robot with good results. During the experimental campaign, temperature dependency of friction coefficients of the robot has been highlighted and quantified.

The results of this work will be used to build a high-fidelity model which can be customized on a specific machine. Such virtual environment could be used both for a more reliable safety assessment of a specific robot application and for a better representation of the behavior of the machine both in nominal and degraded working conditions.

References

1. R. Gentile, D. Bruno, G. Jacazio, M. Sorli, and F. Marino, "Electro-hydraulic servoactuators failure identification: Health features extraction through a high-fidelity physical model," *Int. J. Mech. Control*, vol. 21, no. 1, pp. 91–100, 2020.
2. A. C. Bertolino, M. Sorli, G. Jacazio, and S. Mauro, "Lumped parameters modelling of the EMAs' ball screw drive with special consideration to ball/grooves interactions to support model-based health monitoring," *Mech. Mach. Theory*, vol. 137, pp. 188–210, Jul. 2019.
3. L. A. Grosso, A. De Martin, G. Jacazio, and M. Sorli, "Development of data-driven PHM solutions for robot hemming in automotive production lines," *Int. J. Progn. Heal. Manag.*, vol. 11, pp. 1–13, 2020.
4. S. Mauro, L. S. Scimmi, and S. Pastorelli, "Collision avoidance system for collaborative robotics," *Mech. Mach. Sci.*, vol. 49, no. 3, pp. 344–352, 2018.
5. L. S. Scimmi, M. Melchiorre, S. Mauro, and S. P. Pastorelli, "Implementing a Vision-Based Collision Avoidance Algorithm on a UR3 Robot," *2019 23rd Int. Conf. Mechatronics Technol. ICMT 2019*, pp. 1–6, 2019.
6. Melchiorre, M, Scimmi, LS, Mauro, S, Pastorelli, SP. Vision-based control architecture for human–robot hand-over applications. Asian J Control. 2021; 23: 105– 117.
7. Siciliano, *Robotics: Modeling, Planning, and Control*, vol. 16, no. 4. 2009.
8. M. Gabiccini and A. Bracci, "Explicit Lagrangian formulation of the dynamic regressors for serial manipulators," 2009.
9. M. Neubauer, H. Gattringer, and H. Bremer, "A persistent method for parameter identification of a seven-axes manipulator," *Robotica*, vol. 33, no. 5, pp. 1099–1112, 2015.
10. T. Peters, *Data-driven science and engineering: machine learning, dynamical systems, and control*, vol. 60, no. 4. 2019.
11. F. Piekniewski and I. C. I. S. Member, "Dynamic parameter identification of the Universal Robots UR5."
12. J. Swevers, C. Ganseman, D. Bilgin Tükel, J. De Schutter, and H. Van Brüssel, "Optimal robot excitation and identification," *IEEE Trans. Robot. Autom.*, vol. 13, no. 5, pp. 730–740, 1997.
13. W. Wu, S. Zhu, X. Wang, and H. Liu, "Closed-loop dynamic parameter identification of robot manipulators using modified fourier series," *Int. J. Adv. Robot. Syst.*, vol. 9, 2012.
14. M. Gautier and W. Khalil, "Exciting trajectories for the identification of base inertial parameters of robots," *Int. J. Rob. Res.*, vol. 11, no. 4, pp. 362–375, 1992.
15. G. Antonelli, F. Caccavale, and P. Chiacchio, "A systematic procedure for the identification of dynamic parameters of robot manipulators," *Robotica*, vol. 17, no. 4, pp. 427–435, 1999.
16. W. Rackl, R. Lampariello, and G. Hirzinger, "Robot excitation trajectories for dynamic parameter estimation using optimized B-splines," *Proc. - IEEE Int. Conf. Robot. Autom.*, pp. 2042–2047, 2012.
17. J. Jin and N. Gans, "Parameter identification for industrial robots with a fast and robust trajectory design approach," *Robot. Comput. Integr. Manuf.*, vol. 31, no. July 2019, pp. 21–29, 2015.
18. G. Calefiore, M. Indri, and B. Bona, "Robot dynamic calibration: Optimal excitation trajectories and experimental parameter estimation," *J. Robot. Syst.*, vol. 18, no. 2, pp. 55–68, 2001.
19. N. D. Vuong and M. H. Ang, "Dynamic model identification for industrial robots," *Acta Polytech. Hungarica*, vol. 6, no. 5, pp. 51–68, 2009.
20. J. Jia, M. Zhang, X. Zang, H. Zhang, and J. Zhao, "Dynamic parameter identification for a manipulator with joint torque sensors based on an improved experimental design," *Sensors (Switzerland)*, vol. 19, no. 10, 2019.